International Journal of Scientific Research in Engineering and Management (IJSREM)
Volume: 05 Issue: 05 | May - 2021 ISSN: 2582-3930

A STUDY ON ELECTROCHEMICAL DISCHARGE DRILLING OF SODA – LIME – SILICON- GLASS WITH AID OF MODIFIED SETUP

JYOTHIS P JAYARAJ
Anna university
Department of Mechanical Engineering
Shree Venkateshwara Hi-Tech Engineering College
Eroade,thmilnadu, india

P.LINGESWARAN
Anna university
Department of Mechanical Engineering
Shree Venkateshwara Hi-Tech Engineering College
Eroade,thmilnadu, india

ABSTRACT
The electrochemical discharge machining is integrated by electro-discharge and electro-chemical manufacturing technology. The soda-lime glass is widely used in various fields such as biomedical, optical and industrial industries. Hence, in present study the electrochemical discharge drilling process is applied on soda-lime glass material to find out the material removal rate. The input process parameters are taken as voltage, rotation and electrolyte concentration whereas output response is considered as material removal rate. From this analysis, get the most dominant parameter for material removal rate followed by electrolyte concentration and rotation for soda-lime glass. It is a promising hybrid process for high-performance machining of non-conductive glass. ECDM drilling has been found to have different characteristics and material removal mechanisms in discharge regime. however, these regimes are never separately modeled in existing ECDM models, which leads to large prediction error, especially at low applied voltages and high machining depths. In this paper, a finite element based model for ECDM drilling in discharge regime is presented. Material removal subjected to a single spark was simulated using finite element method.

INTRODUCTION
Electrochemical discharge machining (ECDM) is an emerging non-traditional processing technique that has attracted much research interest in recent years. It involves high-temperature melting and accelerated chemical etching under the high electrical energy discharged on the electrode tip during electrolysis. In ECDM the work piece is merely placed in the close vicinity of the pointed working electrode, and is eroded by sparks jumping across the gas bubbles that develop around the electrode to reach the electrolyte in which everything is immersed, the circuit being completed by the presence of a large counter-electrode. This technology can therefore be equally well use for work pieces made from non-conducting materials such as glass, traditionally difficult to machine, especially at the precision micro level needed for such applications as micro fluidic mixers and reactors. The development of attractive machining technologies such as ECDM is in itself likely to play a decisive part in the growth of micro fluidics-based methods in chemical processing and medical diagnostics.
Among the current micro-machining processes for non-conductive brittle materials, chemical etching can produce micro structures of good shape and accurate dimensions. However, not on the machining speed slow, it also involves complicated procedures and costly equipment, thus limiting its wide application. Laser-beam machining (LBM) can also perform efficient and precise machining, but the high energy density concentrated on the work piece results in micro-cracks and craters as well as cast layer formed ,all of which deteriorate surface quality. Although ultrasonic machining (USM) is well suited for processing hard brittle materials, it has the main drawback of low machining speed. Compared with the above mentioned micro-machining technology

ECDM is not restricted top processing conductive materials and does not require masking when machining semi-conducting materials. Such flexibility and the simple procedure involved in ECDM with great potential in micro-machining of non-conductive hard, brittle materials. ECDM can be used to machine channel like structures and micro holes in glass like materials. Fig. 1.1 shows some work done using

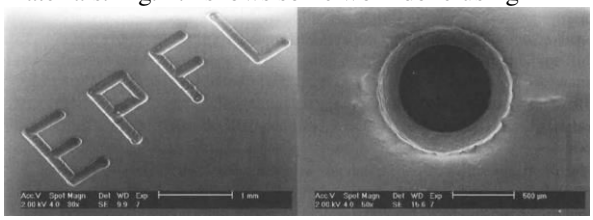

The principle of ECDM is explained in Fig. 1.2. The work piece is dipped in an appropriate electrolytic solution (typically sodium hydroxide or potassium hydroxide). A constant DC voltage is applied between the tool-electrode and the counter-electrode. The tool-electrode is dipped a few millimeters in the electrolytic solution and the counter-electrode is, in general, a large flat plate. The tool-electrode surface is always significantly smaller than the counter-electrode surface. The tool electrode is generally polarized as a cathode, but the opposite polarization is also possible.

The principle of ECDM is explained in Fig. 1.2. The work piece is dipped in an appropriate electrolytic solution (typically sodium hydroxide or potassium hydroxide). A constant DC voltage is applied between the tool-electrode and the counter-electrode. The tool-electrode is dipped a few millimeters in the electrolytic solution and the counter-electrode is, in general, a large flat plate. The tool-electrode surface is always significantly smaller than the counter-electrode surface. The tool-electrode is generally polarized as a cathode, but the opposite polarization is also possible.

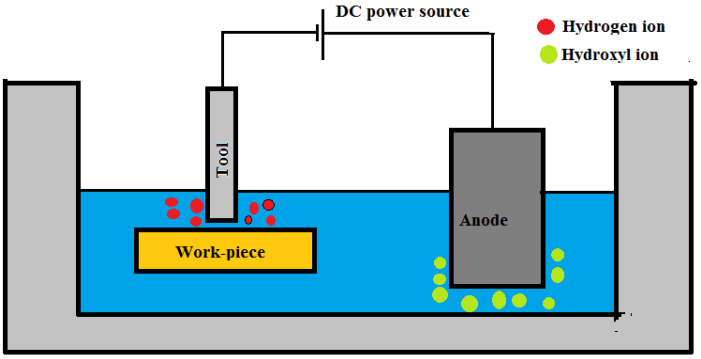

Fig 1.2 Principle of ECDM

When the cell terminal voltage is low (lower than a critical value called critical voltage), traditional electrolysis occurs and hydrogen gas bubbles are formed at the tool-electrode and oxygen bubbles at the counter-electrode depending on their polarization. When the terminal voltage is increased, the current density also increases and more and more bubbles are formed. A bubble layer develops around the electrodes. The density of the bubbles and their mean radius increase with increasing current density. When the terminal voltage is increased above the critical voltage, the bubbles coalesce into a gas film around the tool-electrode. Light emission can be observed in the film when electrical discharges occur between the tool and the surrounding electrolyte. The mean temperature of the electrolytic solution increases in the vicinity of the tool-electrode to about 80-90°C. Machining is possible if the tool-electrode is in the near vicinity of the work piece. However, the gas film around the tool-electrode is not always stable. Micro explosions may occur destroying the machined structure locally. During machining, the local temperature can increase to such an extent, resulting in heat affected zones or even cracking

The advantage of ECDM, compared with other processes is that it can machine conductive/non-conductive, hard/brittle and ductile materials. Initially, this method was attempted to drill on glass substrates, subsequently this method was employed in the drilling of ceramics, composites and stain less steel materials. In order to explore the capabilities of ECDM process, the electrochemical discharge energy was manipulated for the development of ECDM variants like Electro chemical discharge drilling, Electrochemical discharge dressing, etc. By using these variants researchers had been performing various operations like the fabrication of complex and intricate micro profiles, dressing of micro-grinding tools and slicing of glass rods, etc. However, ECDM is also associated with limitation slik below aspect ratio structures, low accuracy etc. To overcome these limitations several external energies have been applied to the ECDM. This resulted in development of several ECDM process variants. Recently, thesimultaneous involvement of these external energies with ECDM process, further developed new triplex hybrid methods. These triplex hybrid methods enhanced the performance meaningfully.

G-ECDM

Grinding assisted electrochemical discharge machining (G-ECDM) is a triplex hybrid machining that combined the effect of electrochemical discharge, mechanical grinding action using a diamond coated tool and electrochemical etching for removal of material from work piece. In G-ECDM, abrasive particles embedded rotary tool (cathode) acts as a grinding tool. The periphery of this grinding tool contains abrasive particle and these abrasive particle layers are bonded using metallic bonding systems. The electrically conductive metallic bond material over the abrasive coated tool generates the spark. Further, this spark energy removes the material from the work surface through melting. Along with this abrasive grinding action, electrochemical etching also removes the material from work surface. Fig. 1.3 shows the schematic view of material removal mechanism for G-ECDM process.

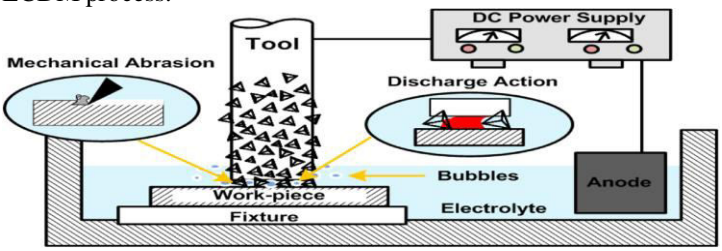

Fig. 1.3 Schematic diagram of G-ECDM

Both the electrodes are dipped in an electrolyte and a pulsed DC voltage will be applied between the electrodes. The electrolysis action at the cathode liberates hydrogen bubbles which will combine to form a gas film at the critical voltage and the film separates the tool from the electrolyte. This will cause high current density at the tool tip and leads to ionization of the hydrogen gas inside the film. An avalanche of electrons which appear as an electric arc strikes the work piece surface placed at the vicinity of discharge. During the spark,

RESEARCH OBJECTIVES

1. To study the effect of process parameters on surface roughness channels machined using G-ECDM on borosilicate glass.
2. To develop a predictive model for surface roughness of fluidic channel machined by G-ECDM
3. To study the surface morphology and properties of fluidic channels machined by G-ECDM on borosilicate glass
4. To study the voltage and current waveforms and effect of inductance on surface roughness during G-ECDM with the help of a modified power supply

3.1 EXPERIMENTAL APPARATUS

To study the effect of parameters on surface roughness, experiments were done using CNC router machine. Some important specification of the machine are listed in the Table 3.1. Diamond coated engraving tool attached to the router spindle and the movement of the tool in 3 axes and rotation of the tool could be controlled using this CNC router. The experimental setup made for G-ECDM is shown in Fig. 3.1.

Table 3.1 Machine specification

odel	NC Router TR 203
ble size	0×1100mm
rking voltage	C 220V, 50/60Hz, Single Phase
indle power motor	5KW, self-coolant Spindle
indle speed	24000rpm
ftware	pe 3, U CAM V9, Art CAM

A customized pulsed DC generator used for providing DC power for the tool and the counter electrode. It has provision to control the frequency and duty ratio. The advantage of using pulsed DC is that it reduces the cracking tendency at higher voltages and will save the energy. Hence for the first experiment this regulated DC power supply is used.

router

CNC

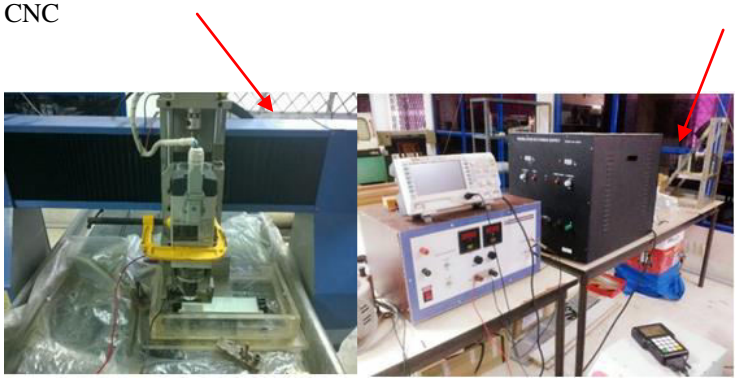

3.2 SELECTION OF TOOL AND WORKPIECE

The tool electrode used in the experiment was diamond coated engraving tool as shown in the Fig 3.2. It was made using the technology called electrolux nickel coating on steel shank. It has an average diameter of 1.96 mm. This diamond coated engraving tool used as cathode and a larger stainless steel plate used as anode. Since the end face of the tool has protruded diamond grits, the necessity to maintain the spark gap is eliminated. The space between grits acts as the sites for spark generation.

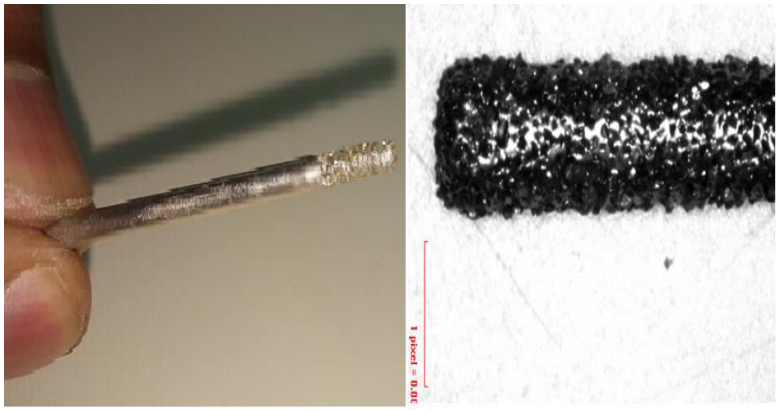

Fig 3.2 Diamond coated engraving tool

The workpieceused was borosilicate glass. Its properties and the chemical composition are listed in Table 3.2 and Table 3.3. Compare to soda lime glass borosilicate glass has excellent thermal properties and strength. It has low thermal expansion coefficient.

Table 3.2 Properties of borosilicate glass

efficient of expansion (/°C)	.5 x 10^{-7}
rain point (°C)	0
neal point (°C)	0
ungs modulus (GPa)	
nsity (g/cm3)	6
ermal Conductivity (W/m-K)	2

Table 3.3 Chemical composition of borosilicate glass

$_2$O	O_2	$_2O_3$	O_3
%	.6 %	3 %	%

3.3 STYLUS PROFILOMETER

The flow parameters like velocity of fluids in a fluidic channel depends on surface roughness of channel surface. Surface roughness of the machined surface is measured using SURFTEST SJ-410 (make: Mitutoyo) with stylus tip diameter of 5µm and cutoff length of 0.8 mm. Fig. 3.3 shows the surface roughness tester used

3.4 OPTICAL MICROSCOPE

Microscopicimages of machined channels gives better understanding about the material removal mechanism.

SELECTION OF TOOL AND WORKPIECE

The tool electrode used in the experiment was diamond coated engraving tool as shown in the Fig 3.2. It was made using the technology called electrolux nickel coating on steel shank. It has an average diameter of 1.96 mm. This diamond coated engraving tool used as cathode and a larger stainless steel plate used as anode. Since the end face of the tool has protruded diamond grits, the necessity to maintain the spark gap is eliminated. The space between grits acts as the sites

4.2 EXPERIMENTAL PROCEDURE

To study the effect of voltage, pulse on time and concentration on surface roughness of G-ECDM machined channels, experiments were carried using the CNC router. The experimental

acrylic sheet in which electrolyte is filled. A steel plate was used as the anode and a diamond coated engraving tool used as the cathode. A customized DC power supply was used to vary the frequency and duty ratio. Work piece of 5mm thickness was immersed in an electrolyte (KOH). A CNC program for machining a channel of 5mm length and 0.5 mm depth was developed in Artcam software which was uploaded to the router. After machining surface roughness of channels machined measured using stylus proflio meter.

4.3 DESIGN OF EXPERIMENTS

Three level full factorial experimental design (3^3= 27 runs) was selected. The factors selected were voltage, pulse on time and electrolyte concentration. The selected factors and their levels are shown in the Table 4.1. The response measured was surface roughness (Ra value). Analysis of variance. A regression model was developed to predict the surface roughness of machined surface.

Table 4.1 List of factors and level

ıctors	**ɔtations**	**ıit**	**ɛvels**		
ɔltage			)	)	)0
ılse on time			)004	)005	)006
ncentration					

4.4 RESULTS AND DISCUSSION

4.4.1 Full factorial experimental results

The main effect plot obtained for surface roughness is shown in Fig. 4.1. The main effect plot gives an average value of response obtained from each level of parameters. The main effect plot shows that as voltage increases, Ra value increases. It is due to the fact that increase in voltage increases energy supplied by the spark which leads to the formation of craters with more depth. More irregular deep craters produces higher Ra values and hence a poor surface finish. When pulse on time increases, the energy will be supplied for more time in a given pulse cycle. This will increase the volume of craters produced thereby increasing the Ra value. When concentration of electrolyte increases, chemical etching process become predominant and it will smoothen the irregularities. This will reduce the Ra value.

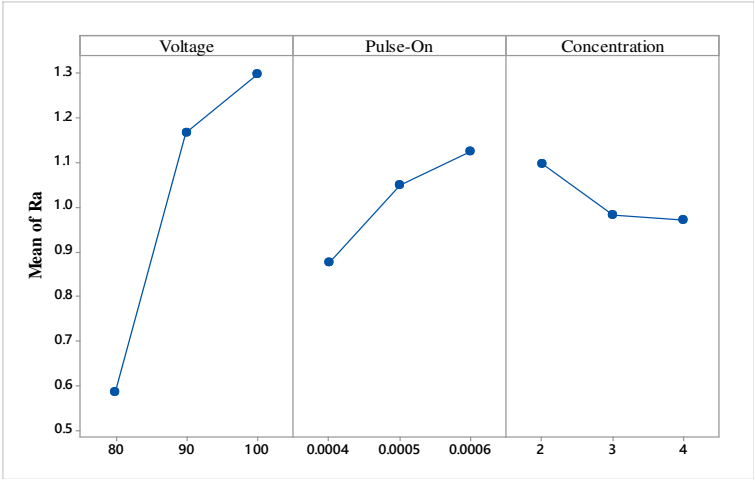

Fig. 4.1 Main effect plot for *Ra* value

4.4.2 Results of Analysis of Variance

Interaction effects of pulse-on time and concentration was also found to be significant. The interaction plot for pulse-on time and concentration is shown in Fig. 4.2.

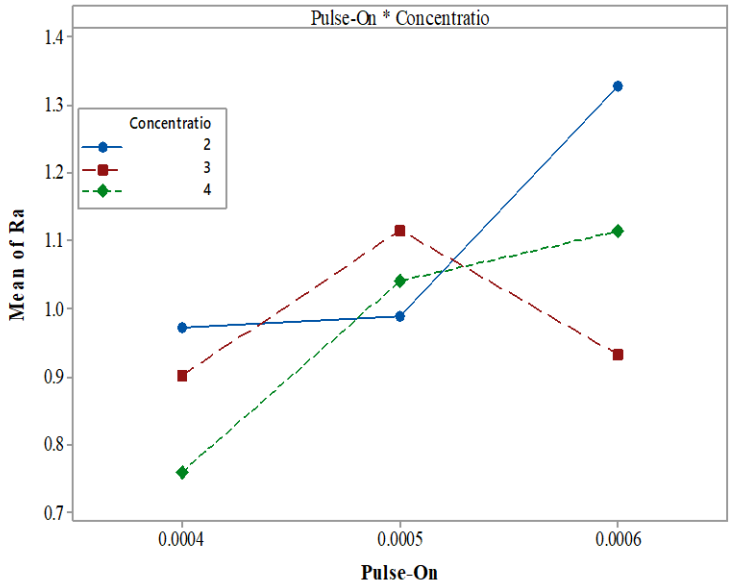

Fig. 4.2 Interaction plot for pulse on time and

4.5 HARDNESS STUDY OF G-ECDM MACHINED SURFACE

Hardness of fluidic channel machined using G-ECDM and of parent material (borosilicate glass) are measured using micro indentation hardness tester. The load applied was 2 Kgf for 20s dwell time. Fig 4.3 shows the indention produced in both machined and parent material surface.

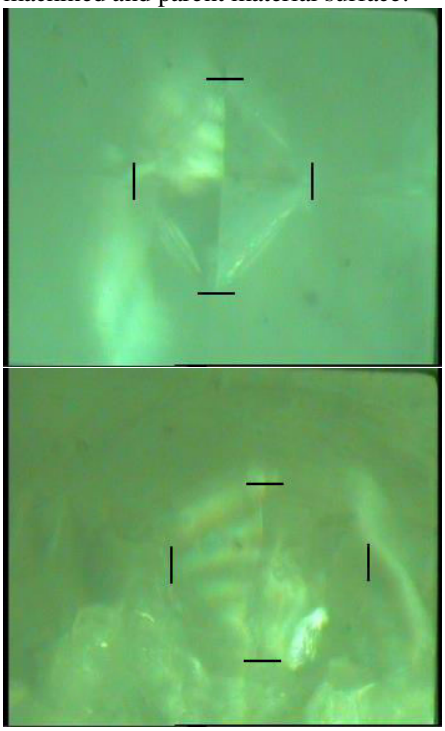

Fig 4.3 Indentation produced in parent material and machined surface

Vickers hardness number of G-ECDM machined surface measured as 748.92 HV and for borosilicate glass without machining measured as 689.09 HV. The increase in hardness in case G-ECDM machined surface is due to the recast layer formation at the time of machining. Table 4.4 shows the result obtained from the hardness test.

Table 4.4 Results of hardness test

	orosilicate glass without machining	achined surface
	Kg	Kg
	.65 µm	.86 µm
	.09 µm	.65 µm
hardness No.	9.1 HV	8.92 HV

STUDY OF VOLTAGE AND CURRENT WAVEFORMS

To obtain the voltage and current wave forms for the ECDM and G-ECDM, a circuit is designed as shown in Fig.5.1. A differential probe is connected with the oscilloscope to obtain the voltage wave form and incase of current wave form a current probe is connected. Tool used for ECDM, G-ECDM are stainless steel needle and diamond coated engraving tool respectively. 4M KOH solution was used as the electrolyte. The experiment was carried out in constant voltage of 60 V. The oscilloscope used have a provision to quantify the amplitude and frequency of wave obtained. A bridge rectifier is used to convert the AC to DC

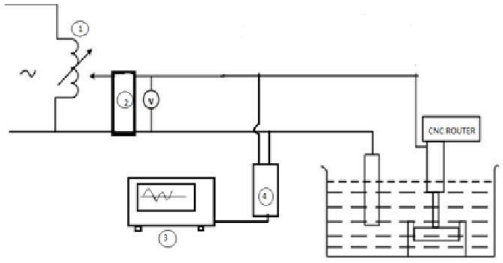

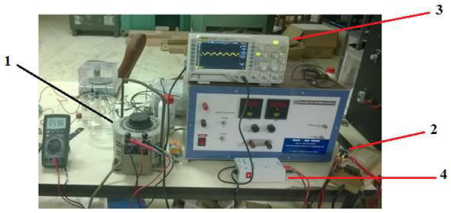

acrylic sheet in which electrolyte is filled. A steel plate was used as the anode and a diamond coated engraving tool used as the cathode. A customized DC power supply was used to vary the frequency and duty ratio. Work piece of 5mm thickness was immersed in an electrolyte (KOH). A CNC program for machining a channel of 5mm length and 0.5 mm depth was developed in Artcam software which was uploaded to the router. After machining surface roughness of channels machined measured using stylus proflio meter.

4.3 DESIGN OF EXPERIMENTS

Three level full factorial experimental design (3^3= 27 runs) was selected. The factors selected were voltage, pulse on time and electrolyte concentration. The selected factors and their levels are shown in the Table 4.1. The response measured was surface roughness (Ra value). Analysis of variance. A regression model was developed to predict the surface roughness of machined surface.

Table 4.1 List of factors and level

actors	**otations**	**nit**	**evels**		
oltage					0
lse on time			0004	0005	0006
ncentration					

4.4 RESULTS AND DISCUSSION

4.4.1 Full factorial experimental results

The main effect plot obtained for surface roughness is shown in Fig. 4.1. The main effect plot gives an average value of response obtained from each level of parameters. The main effect plot shows that as voltage increases, Ra value increases. It is due to the fact that increase in voltage increases energy supplied by the spark which leads to the formation of craters with more depth. More irregular deep craters produces higher Ra values and hence a poor surface finish. When pulse on time increases, the energy will be supplied for more time in a given pulse cycle. This will increase the volume of craters produced thereby increasing the Ra value. When concentration of electrolyte increases, chemical etching process become predominant and it will smoothen the irregularities. This will reduce the Ra value.

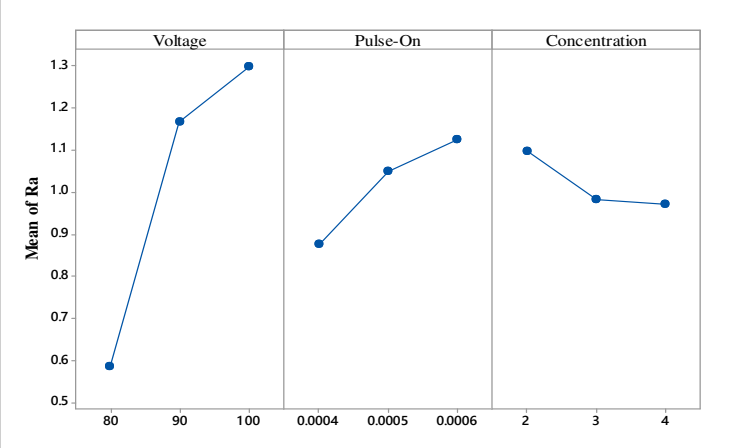

Fig. 4.1 Main effect plot for *Ra* value

4.4.2 Results of Analysis of Variance

Interaction effects of pulse-on time and concentration was also found to be significant. The interaction plot for pulse-on time and concentration is shown in Fig. 4.2.

CHAPTER 5
STUDY OF VOLTAGE AND CURRENT WAVEFORMS

5.1 INTRODUCTION

From literature survey, several researchers proposed mechanism behind ECDM process. For better understanding about the mechanism a study of voltage and current waveform is carried out. An experiment was conducted to revel the temperature rise and material removal. Based on the experimental observation of time varying voltage and current, mechanism for electrochemical discharge is explained. A comparison of ECDM and G-ECDM also carried out based on the voltage waveforms of both the process at same working condition.

5.2 EXPERIMENTAL PROCEDURE

To obtain the voltage and current wave forms for the ECDM and G-ECDM, a circuit is designed as shown in Fig.5.1. A differential probe is connected with the oscilloscope to obtain the voltage wave form and incase of current wave form a current probe is connected. Tool used for ECDM, G-ECDM are stainless steel needle and diamond coated engraving tool respectively. 4M KOH solution was used as the electrolyte. The experiment was carried out in constant voltage of 60 V. The oscilloscope used have a provision to quantify the amplitude and frequency of wave obtained. A bridge rectifier is used to convert the AC to DC

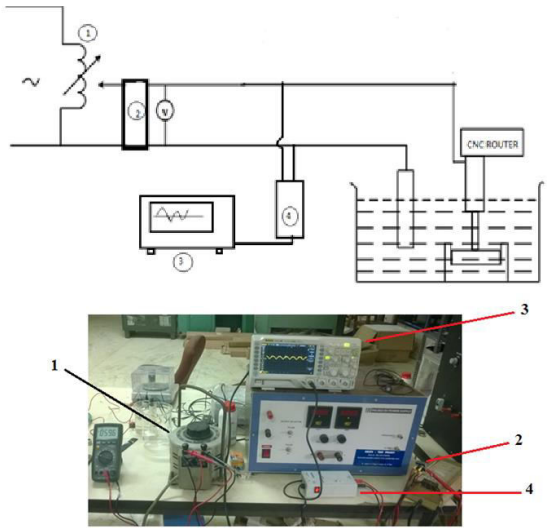

1.Auto transformer
2.Bridge rectifier
3.Oscilloscope

5.3 OBSERVATIONS AND DISCUSSION

Voltage wave form for ECDM and G-ECDM were obtained as shown in Fig.5.2.and Fig 5.3. This figure shows that the spark ignition delay is occurred in the ECDM process but not in the G-ECDM process.

Fig. 5.1 Circuit for waveform study

Fig. 5.2 Voltage waveforms (a) ECDM (b) G-ECDM

In EDM process ignition delay are considered due to the abnormal arcing. The abnormal arc position occurs at more or less at the same spot. Hence abnormal arc will continues to remove materials from same position it will leads to a burnedmachined surface and critical tool wear.

(b)

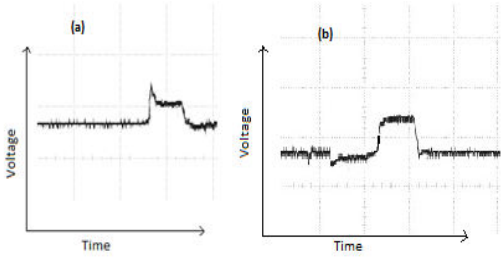

Fig. 5.3 Peak areas of voltage waveform in ECDM and G-ECDM

Fig. 5.3 Peak areas of voltage waveform in ECDM and G-ECDM

Even though G-ECDM waveform resembles that EDM abnormal acting, the craters produced in the G-ECDM surface are distributed randomly over the machined surface. That means arcing did not occurred at same locality. The absence of ignition delay in G-ECDM means relatively long arc maintaining period occurs, hence more MRR is obtained. Moreover a stable processing condition is obtained.

For each pulse cycle, the arc maintaining time tm is given by

$t_m = t_t - t_d$ (5.1)

Where t_t is the total pulse duration time in one cycle and td is the ignition delay time. Accordingly, the arc energy can be determined by

$E = \int_0^{tm} VIdt$ (5.2)

Where V is the arc maintaining voltage and I is the arc current. For the case of G-ECDM, since there is no ignition delay, arc energy will be high. Hence the MRR in case of G-ECDM will be higher.

The current waveform obtained for G-ECDM process shown in the Fig.5.4. Large spikes are seen at the time of each discharge. Discharge frequency or the rate of discharge occurring at the cathode tip can be estimated by taking the reciprocal of the total time duration (pulse duration and delay b

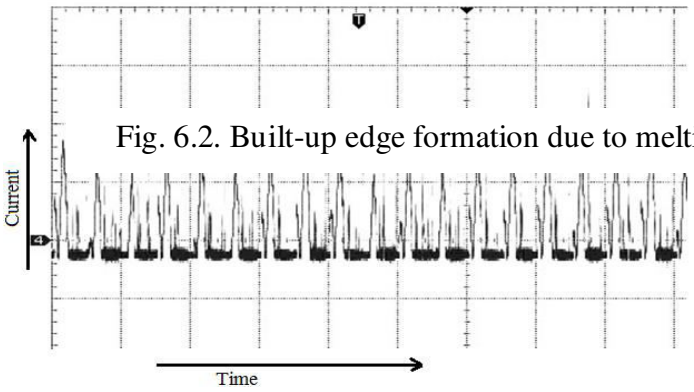

Fig. 5.4 Current waveform of G-ECDM

The current waveforı
the Fig.5.4. Large sp
Discharge frequency or the rate of discharge occurring at the cathode tip can be estimated by taking the reciprocal of thetotal time duration (pulse duration and delay between consecutive pulses). When a DC voltage is greater than the critical voltage that needed to produce the discharge is applied to ECDM cell, electrolysis reaction take place. Reduction of electrolyte at cathode results in hydrogen gas bubbles. These bubbles get accumulated at the cathode tip immersed in electrolyte. Bubble generation goes on increasing, leading to combining of bubbles into a single large bubble which isolate the tip completely from the electrolyte. When an isolating film of hydrogen gas bubbles covers the cathode tip portion in the electrolyte, the tip is covered by a gaseous layer. At this time a large dynamic resistance is present and the circuit current becomes almost zero.

A high electric field of the order 10V/µm gets generated at the cathode tip and it causes generation of arc discharge. At the instant when discharge occurs, a large number of electrons generated by ionization, flows toward the anode. It leads to a sudden increase in the current. These currents spikes are shown in the Fig. 5.3. These peaks have very short duration of time.

6.2 RELATION BETWEEN Ra AND Rt

In G-ECDM, thermal energy of spark is used to remove the material in the form of craters by melting and vaporization. The volume of craters depend upon the energy of the spark. Some portion of molten materials form a built up edge around the craters as shown in Fig. 6.2. This is the case of single spark. After the occurrence of several discharges, the craters overlap and sharp peaks would be formed. Due to mechanical grinding action the sharp portions will be removed and a better surface will be obtained (Fig 6.3). The average roughness value Ra is given by the average crater height of the overlapped craters. With the aid of a stylus profilometer, the Ra and Rt value of the channels are measured. A relation between Ra and Rt is obtained from the graph of Ra VsRt as shown in Fig. 6.4.

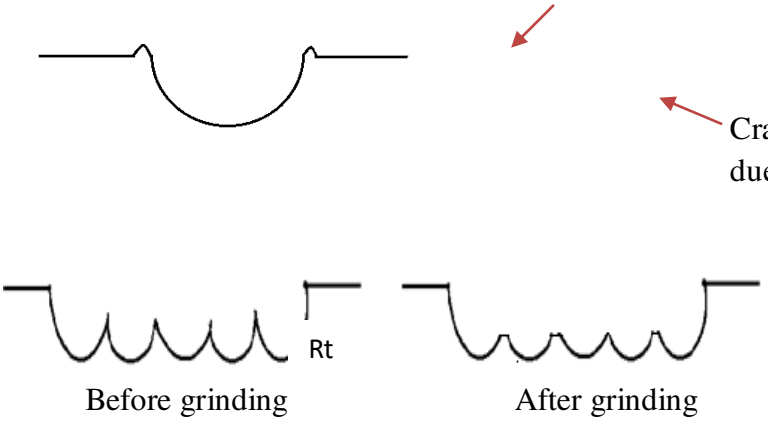

Fig. 6.2. Built-up edge formation due to melting

Fig. 6.3. Overlapped craters before and after grinding

e between highest peak and lowest valley. From the observed data, a numerical relation between *Ra* and *Rt* is developed which is given by (6.1)

$Ra = 1/8.5\ (Rt)$ (6.1)

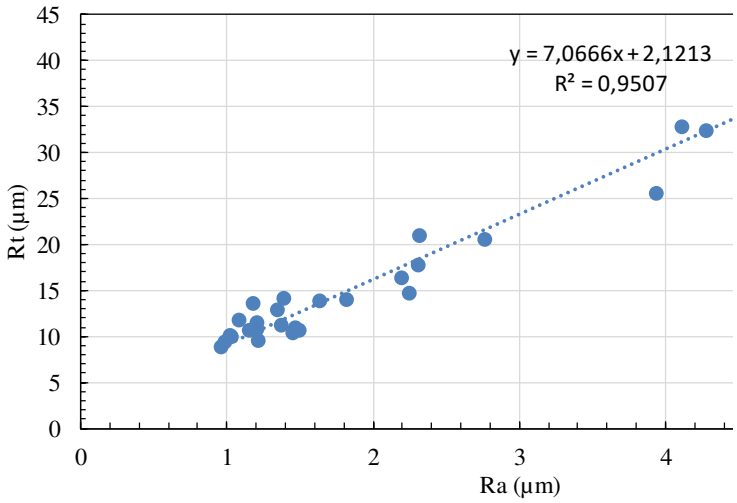

6.3 MODELING OF SURFACE ROUGHNESS IN G-ECDM

The arc energy produced can be determined by the following equation

$E_a = \int_0^{tm} VIdt$ (6.2)

Where t_m is the arc maintaining time, V is the arc maintaining voltage and I is the arc current. The volume of crater produced (V_c) by a spark is proportional to the arc energy produced.

$V_c \alpha E_a$

Basak et al. [6] found experimentally a relation connecting volume of the material removed per spark and the energy supplied per spark as follows.

$V_c = 0.7 \times 10^{-5} E_a^{1.5}$ (6.3)

Thermal energy of spark will be used to remove the material in the form of micro crater. Assumed that the crater formed in the shape of spherical cap. The removed molten material forms a build-up- edge (BUE) around the crater as is the depth of crater and 'a' is the radius of

Volume of the crater produced by single spark can be obtained by using the given equation

$V_c = \frac{\pi H}{6} + (3a^2 + H^2)$ (6.4)

Jiang et al. [12] found that the ratio of crater depth to the crater diameter is in the range 0.2 to 0.3. Hence the above equation become

$V_c = \frac{\pi H}{6} + 13H^2$ (6.5)

Comparing Eq. (6) and Eq. (4), and we will get

$\frac{\pi H}{6} + 13H^2 = 0.7 \times 10^{-5} E_a^{1.5}$ (6.6)

From the above equation we can obtain the value of H. From microscope observation, the value of average peak to valley distance is found to be 1/4th of H. So Surface roughness R_a can be expressed as a function of arc maintaining voltage, arc current and arc maintaining time.

EFFECT OF INDUCTANCE ON SURFACE ROUGHNESS AND OVERCUT

7.1 INTRODUCTION

If a changing flux is linked with a coil of a conductor there would be an emf induced in it. The property of the coil of inducing emf due to the changing flux linked with it is known as inductance of the coil. Due to this property all electrical coil can be referred as inductor. In other way, an inductor can be defined as an energy storage device which stores energy in form of magnetic field. In the case of G-ECDM this stored energy causes variation in energy of discharge. From literature survey some preliminary studies carried in this area and found out that circuit inductance have effect on material removal rate. In this chapter the effect of external inductance on surface roughness and overcut of fluidic channe

7.2 EX

An autotransformer was used as the variable inductor for the experiment. Value of inductance at different position of autotransformer pointer found out using a LCR meter. Fig 7.1 shows the autotransformer which is used as the variable inductor.

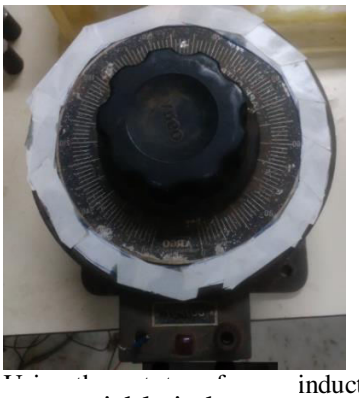

Fig 7.1 Autotransformer as variable inductor

inductance can be varied in the range
ble 7.1 shows values of inductance at different voltage position of autotransformer. A modified circuit designed for conducting experiment as shown in the Fig. 7.2. It consist of a bridge rectifier to covert AC to DC, a primary autotransformer for adjusting the voltage and a secondary autotransformer which is functioning as a variable inductor. A voltmeter connected to the primary autotransformer measures the voltage applied for the process. This modified circuit connected to the G-ECDM setup.

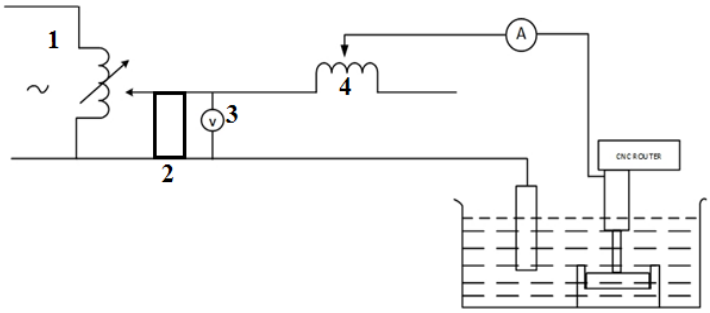

1. Autotransformer
2. Bridge rectifier
3. Voltmeter
4. Variable inductance

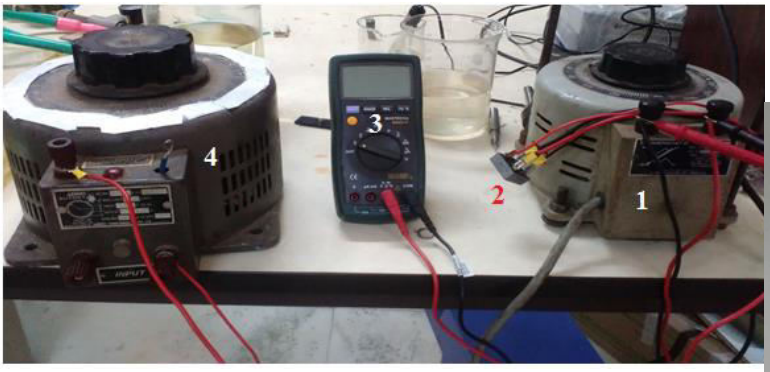

Fig 7.2 Circuit for studying effect of inductance

Two different tools were used for the experiment. A diamond coated engraving tool which is similar to the tool used for the previous experiment and a diamond coated drill bit of diameter 6 mm. Fig 7.3 shows the tools were used. Movement of the tool controlled using the CNC router. Two different CNC programs were developed for two different tools using artcam software. KOH at different concentration used as the electrolyte

Table 7.1 Values of inductance at different voltage position

ltage position (V)	**ductance (mH)**
0	0
0	8
0	6
0	0
0	2

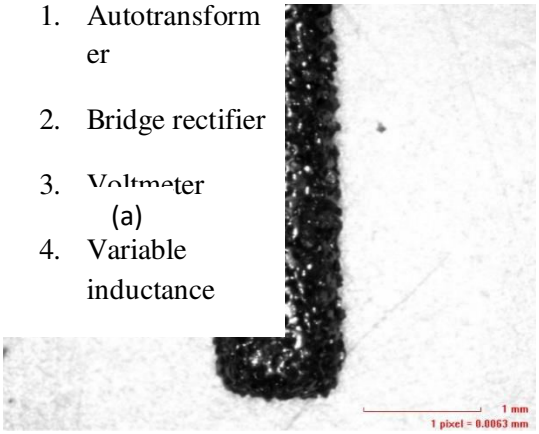

(a) (b)

Fig. 7.3 G-ECDM tools (a) diamond coated engraving tool (b) core drill bit

To study the effect of inductance on surface roughness and overcut of fluidic channels machined using the diamond coated engraving tool, the process parameters selected for the experiments are given in the table 7.2. Box-Behnken design is used to performing the experiments. For three factors, the Box-Behnken design offers some advantage in requiring a fewer number of runs. The number of runs in the experiment reduced to 15.

Table 7.2 Process parameters and their levels

ıctors	**ɔtations**	**ıit**	**evels**	
ɔltage				
ductance		H		
ncentration				

7.3 RESULTS

The experiments are conducted by using diamond coated engraving tool and fluidic channels of depth 0.5mm are made on borosilicate glass for the various combination of the process parameters

G-ECDM machined fluidic channel using diamond coated engraving tool are shown in the Fig. 7.4. Surface roughness of the channels are machined using Surftest SJ- 410 profilometer. A diamond stylus of 5µm tip radius with cut off length of 2.5mm with stylus speed of 0.5mm/s. The over cut of the channels measured using optical microscope. The microscopic images of the fluidic channels are shown in the Fig. 7.5

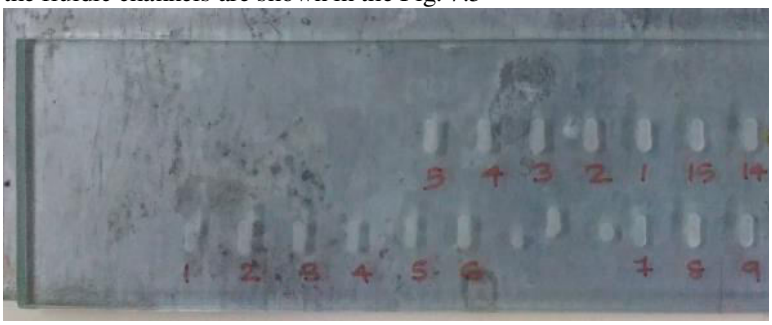

Fig 7.4 Fluidic channels machined using G-ECDM

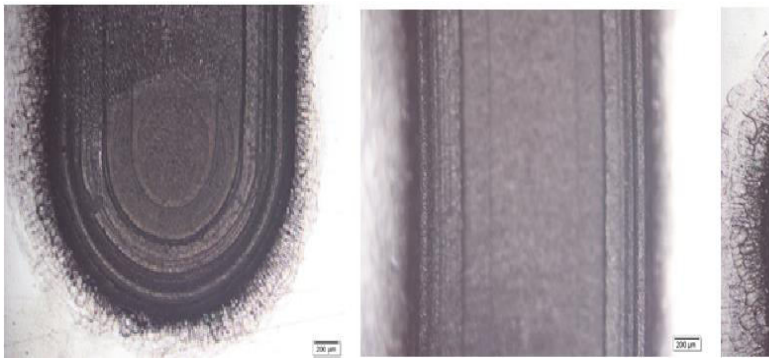

Fig 7.5 Optical microscopic images of fluidic channels

7.4. Response prediction using artificial neural network (ANN)

A neural network is a computing technique which can be used for data regression and prediction. It is similar to brain's structure. A neural network is a computing system which can be effectively used for data regression and prediction. Neural network is made up of a number of simple and highly interconnected nodes or processing elements called neurons. The goal of neural network is to map a set of input patterns onto a corresponding set of output patterns. The neural network achieves this mapping by first training the neurons to be suitable for a given series of patterns. Then, the neural network applies this model to a new input pattern to predict the appropriate output pattern. There are many kinds of neural networks depending on their structure, function, or training methods. In this study, a typical feed forward neural network with a back propagation learning algorithm is used to train it. The input vector and output vectors are correlated using a transfer function. Different kinds of transfer functions are there, and a hyperbolic tangent function is selected for this study.

"Visual gene developer 1.7" is used to train the input data and infer the results for test data. Fig. 7.6 shows the neural network architecture. A back propagation neural network with 3 input neurons, two hidden layers and 1 output neuron has been used. First hidden layer consist of 10 neurons and second with 5 neurons.

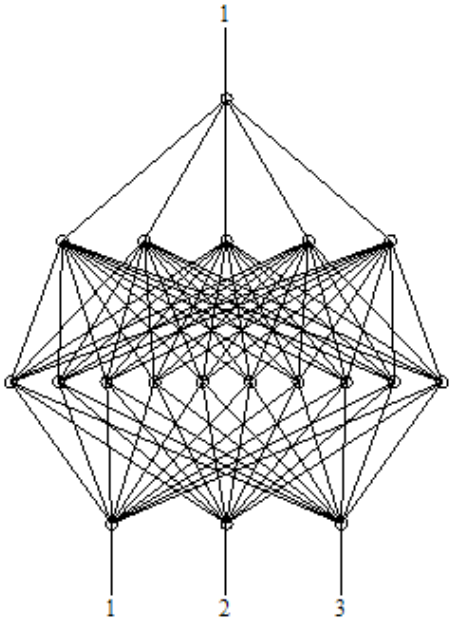

Fig 7.6 Neural network architecture

A learning rate of 0.01 and momentum factor of 0.1 have been used. 100001 cycles of iterations have been performed. The training data and testing data have been normalized so that inputs and outputs are within the range of 0-1. Once the network is trained with the given training data, the values are inferred both for training and testing the data. Fig. 7.7 shows the comparison of performance of the neural network and regression model for the output for training data. It is seen that, the inferred values by using neural network are very close to the actual values. ANN was able to predict the response (surface roughness) with a mean error of 2.52%. Six treatment combinations are used for checking the significance of the regression model and ANN model. Table 7.6 shows the comparison of experimental results, ANN predicted surface roughness (Ra) and regression model predicted surface roughness for testing data. For all treatment combinations, ANN was able to predict the Ra value with less error when compared to that predicted by regression model.

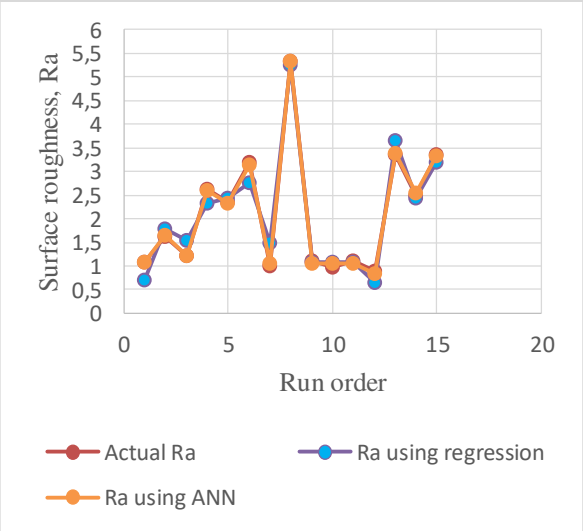

Fig 7.7 Comparison of actual Ra, Ra predicted by regression model and Ra predicted using ANN

7.5 G-ECDM USING DIAMOND CORE DRILL BIT

Diamond core drill bit which shown in the Fig.7.1 generally using for drilling holes in composite materials. Due to its abrasive coating on the edge surface it can be used as a G-ECDM tool also. A core drill bit of 6mm used for making channels on borosilicate glass with different process parameters. Machining of channels using diamond core drill bit is shown in Fig 7.7. The parameters used and their different values are shown in the table 7.7

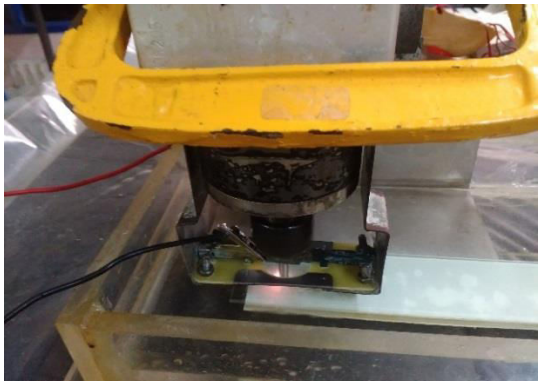

(a)

Table 7.3 Parameters and their levels for the experiment with core drill bit

Voltage	Concentration	Inductance
70	3	70
80		
90		
100		
90	3	70
	4	
	5	
	6	
90	3	40
		70
		100
		130

7.5.1 Results and discussion

Compare to diamond coated engraving tool core drill bit have more diameter, hence critical voltage for G-ECDM using core drill bit is more. Challenge faced during G-ECDM using core drill bit is that, due to its higher critical voltage chance of work piece (borosilicate glass) is more. Using diamond core drill bit, 0.5 mm depth and 12mm length channels were made in borosilicate glass. Fig 7.7 shows the channels obtained with different values of parameters. Surface roughness value of every channel measured using stylus profilometer with 5µm stylus and 2.5mm sampling length. Individual effects of each parameters on surface finish is studied.Table 7.8 shows results of the experiment carried using diamond core drill bit

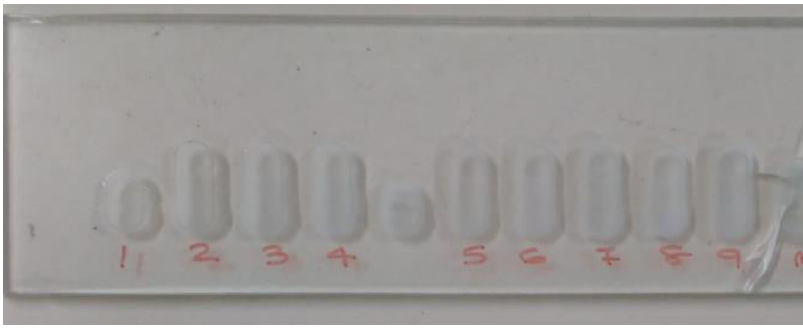

Fig. 7.10 G-ECDM using diamond core drill bit

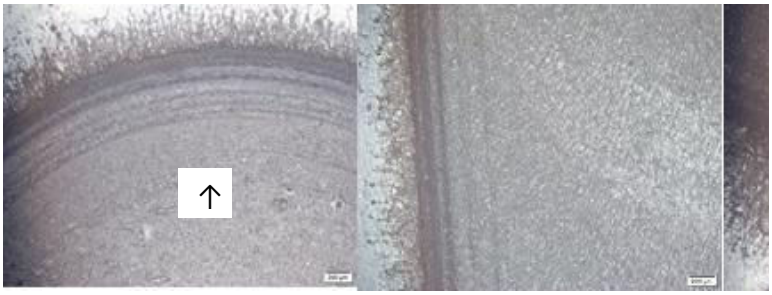

(b)

Fig. 7.11 (a) machined channels (b) microscopic

Table 7.4 Results of experiment with core drill bit

oltage (V)	urface roughness, Ra (µm)
)	452
)	722
)	237
0	193
oncentration (M)	a (µm)
	237
	325
	118
	425
ductance (mH)	a (µm)
)	765
)	237
0	328
0	425

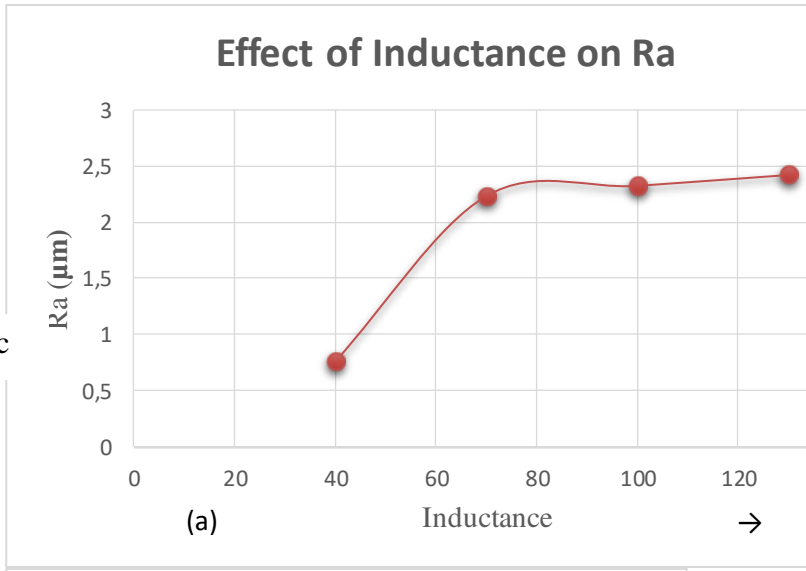

(a)

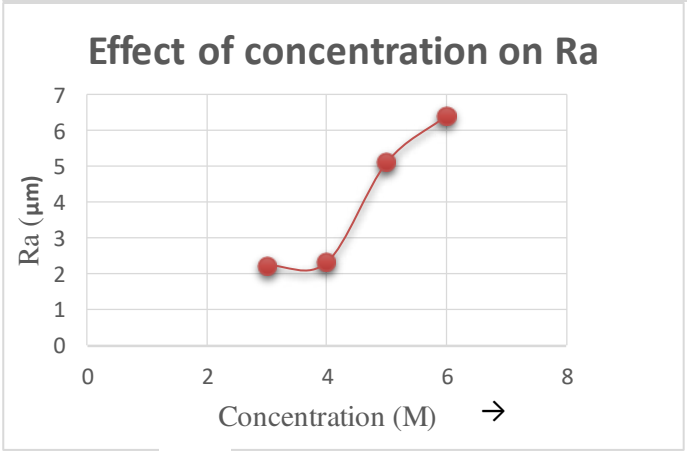

(b)

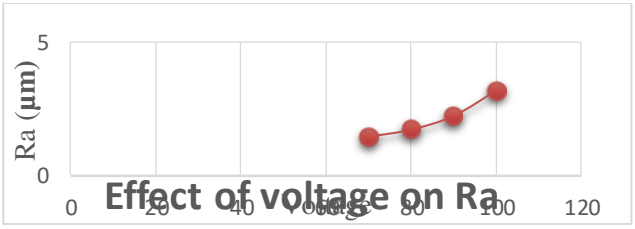

Fig 7.12 Variation of surface roughness with parameters (a) Inductance Vs Ra (b) Concentration Vs Ra (c) Voltage Vs Ra

7.5.2 Effects of parameters on surface roughness

According to the results graphs were plotted for each parameters verses surface roughness (Fig 7.8). The graphs shown that almost a similar result to the G-ECDM with diamond coated engraving tool. In case of inductance effect on surface finish diamond coated engraving tool showed a trend like first decreasing up to a point then increasing. But this trend is not shows in case of diamond core drill bit. Here roughness value is increases with increase in circuit inductance value. For concentration and voltage its shows similar trend with experiment with diamond coated engraving tool.

CC

CONCLUSIONS AND SCOPE OF FUTURE WORK

8.1 CONCLUSIONS OF STUDY

Fluidic channels of average width 2 mm machined on borosilicate glass with G-ECDM process using diamond coated engraving tool and the following conclusions are made.

- Effects of parameters (concentration, pulse on time and voltage) on surface finish of machined surface is studied and it is found that surface finish is more at lower voltage and lower pulse on time
- It assured that Ra value increase from 0.6µm to 1.3µm for an increase in voltage from 80V to 100V and it is due to when voltage increases, energy supplied per spark increases hence more craters are produced
- The decrease in roughness value around 13.5% is will be an increase in concentration from 2M to 4M, and it is due to chemical etching reaction increases with concentration and it causes smoothing of sharp edges
- The recommended parameters conditions are lower voltage, lower pulse on time and higher concentration
- Hardness of machined surface wil be G-ECDM machined surface have more hardness compare to the parent material and it is due to the recast layer formation during machining

A circuit is which to study the voltage and current waveform in G-ECDM and ECDM that will be shows by different study that

- Using voltage waveforms of ECDM and G-ECDM a comparison of both process is carried and its explained MRR is more in G-ECDM
- Using current waveform of G-ECDM, mechanism behind the material removal in G-ECDM is explained
- A mathematical model developed to predict the surface roughness of surface machined using G-ECDM

A modified circuit can be develop to study the effect of external inductance on surface roughness and overcut of fluidic channels machined using G-ECDM and effects of parameters (inductance, voltage and concentration) on surface roughness and overcut of fluidic channel is studied. From the experimental study the following conclusions are made

- We study that when inductance increases surface roughness first decreases up to a point and then increases. It is due to more inductance cause more energy stores in the circuit and this energy will utilize for the generation of discharge. Hence more craters will forms and surface roughness increases
- When voltage and concentration increase it is found that surface roughness and overcut are also increases
- A statistical model is developed to predict the surface roughness and overcut of channels in terms of inductance voltage and concentration
- 6mm width channels machined in borosilicate glass using diamond core drill bit and its performance compared with G-ECDM using diamond coated engraving tool. It is found that at same working conditions G-ECDM with diamond core drill bit gives better surface finish than the other.

8.2 SCOPE OF FUTURE WORK

- Detailed study on the hardness variation of G-ECDM machined surface
- Possibility of applying G-ECDM to other advanced ceramics
- Development of a set up for G-ECDM with internal electrolyte flushing

REFERENCES

[1]Liu, J. W.,Yue, T. M., and Guo, Z. N., 2013, "Grinding-Aided Electrochemical Discharge Machining Of Particulate Reinforced Metal Matrix Composites," Int. J. Adv. Manuf. Technol., **68**, pp. 2349–2354

[2] Chak, S. K., and VenkateswaraRao, P., 2007, "Trepanning Of Al_2O_3By Electro-Chemical Discharge Machining (ECDM) Process Using Abrasive Electrode With Pulsed DC Supply," Int. J. Mach. Tools & Manuf., **47**, pp. 2061–2070

[3] Zheng, Z. P., Hsu, Y. S., Huang, F. Y., and Yan, B. H., 2007, "Feasibility of 3D Surface on Pyrex Glass by Electrochemical Discharge Machining (ECDM)," Proc. AEMS07., **28**, pp. 198-207

[4] Kolhekar, K. R., Sundaram, M., 2016, "A Study on the Effect of Electrolyte Concentration on Surface Integrity in Micro Electrochemical Discharge Machining," Procedia CIRP., **45**, pp. 355 – 358